KA-TP-11-2007

Irreducible three-loop contributions to the pressure in Yang-Mills thermodynamics

Dariush Kaviani[†] and Ralf Hofmann[*]

[†] *Institut für Theoretische Physik*
Universität Heidelberg
Philosophenweg 16
69120 Heidelberg, Germany

[*] *Institut für Theoretische Physik*
Universität Karlsruhe (TH)
Kaiserstr. 12
76131 Karlsruhe, Germany

Abstract

In the effective theory for the deconfining phase of SU(2) Yang-Mills thermodynamics we compute estimates for the moduli of the irreducible three-loop diagrams contributing to the pressure. Our numerical results are in agreement with general expectations.

1 Introduction

To obtain essential analytical insights into the thermodynamics of four-dimensional Yang-Mills theories is difficult even at high temperature where gauge fields do propagate. A perturbative treatment of Yang-Mills thermodynamics, which is technically highly involved, runs into problems that are associated with the masslessness of the fundamental, propagating degrees of freedom. A manifestation of this problem is the apparent nonconvergence of the perturbative series[1] which can be pinned down to the weak screening in the magnetic sector of the theory [3]. Loosely speaking, this problem arises because the perturbative a priori estimate for the thermal ground state is inappropriate. Namely, the presence of topologically nontrivial fluctuations, which do contribute to the thermodynamics of the Yang-Mills system[2] in a direct (ground state) and indirect (masses) way, is neglected in perturbative loop expansions.

In [6] a nonperturbative approach to SU(2) and SU(3) Yang-Mills thermodynamics is developed. Let us discuss the deconfining phase for the SU(2) case only. The idea is to first derive a thermal ground state which is composed of interacting topological fluctuations: calorons and anticalorons. While the dynamics of these fluctuations would appear to be highly complex in the hypothetic case, where an externally provided probe of a given momentum transfer is applied to the system, the case of pure, infinite-volume thermodynamics[3] selfconsistently adjusts a maximal resolution $|\phi|$ in such a way that the ground state admits a remarkably simple analytical description. To derive this situation a spatial coarse-graining needs to be performed which yet turns out to be sufficiently local to only require consideration of calorons and anticalorons of topological charge modulus $|Q| = 1$ [7]. As a consequence, an adjoint and inert (spatially homogeneous) scalar field ϕ emerges which together with a pure-gauge (coarse-grained) configuration describes the ground state of the system, see also [8]. The presence of ϕ signals a dynamical gauge-symmetry breaking SU(2)→U(1) implying that two out of the three propagating and coarse-grained gauge-mode species acquire a (temperature-dependent) mass. This and the fact that the off-shellness of these modes and the momentum transfer in local vertices is highly constrained after spatial coarse-graining imply the rapid convergence of loop expansions in the effective theory [9]. The purpose of the present article is to demonstrate this by estimating the irreducible three-loop contribution to the pressure in deconfining SU(2) Yang-Mills thermodynamics.

The paper is organized as follows. In Sec. 2 we briefly review technical essentials of the effective theory. Sec. 3 first explains what is meant by the term 'irreducible

[1] At $T = 0$ it is suggestive that the perturbative series represents an asymptotic expansion, and so the first few orders do capture a great deal of the physics [1, 2]. The perturbative series at finite temperature apparently does not enjoy this property.

[2] For example, the trace of the energy-momentum tensor rises linearly with temperature [4], and the dimensionally reduced theory confines [5].

[3] Subject to two scales only: temperature T and Yang-Mills scale Λ.

diagram' according to the discussion in [9]. Subsequently, we elucidate the structure of irreducible three-loop diagrams. In Sec. 4 we perform the integrations numerically using the Monte-Carlo method. Results are indicated and discussed. Finally, Sec. 5 gives our conclusions.

2 Effective theory for deconfining phase

Here we very briefly review the effective theory for SU(2) Yang-Mills thermodynamics being in its deconfining phase. The following effective action emerges upon a self-consistent spatial coarse-graining involving interacting nontrivial-holonomy calorons of topological charge modulus $|Q| = 1$ (ground state) and topologically trivial gauge fields (excitations) [6]:

$$S = \mathrm{tr} \int_0^\beta d\tau \int d^3x \left(\frac{1}{2} G_{\mu\nu} G_{\mu\nu} + D_\mu \phi D_\mu \phi + \Lambda^6 \phi^{-2} \right) . \tag{1}$$

In Eq. (1) $G_{\mu\nu} \equiv G^a_{\mu\nu} \frac{\lambda^a}{2}$, $G^a_{\mu\nu} = \partial_\mu A^a_\nu - \partial_\nu A^a_\mu + e\, \epsilon^{abc} A^b_\mu A^c_\nu$, and $D_\mu \phi = \partial_\mu \phi + ie[\phi, A_\mu]$ where A_μ is the (coarse-grained) gauge field of trivial topology, and e denotes the effective gauge coupling.

In a first step, only a noninteracting (trivial-holonomy) caloron and anticaloron is coarse-grained over an infinite spatial volume into the phase of a spatially homogeneous adjoint scalar field ϕ. Subsequently, the presence of a Yang-Mills scale Λ is assumed[4] to obtain the modulus $|\phi| = \sqrt{\frac{\Lambda^3}{2\pi T}}$. The latter determines the finite spatial length scale $|\phi|^{-1}$ at which the above coarse-graining saturates. Taking interactions between calorons and anticalorons into account, a (coarse-grained) pure-gauge configuration emerges. Going from a gauge, where ϕ winds along the compactified euclidean time dimension, to unitary gauge[5] we arrive at

$$\mathcal{L}^{u.g.}_{\mathrm{eff}} = \mathcal{L}\left[a_\mu\right] = \frac{1}{4} \left(G^{a,\mu\nu}_E[a_\mu]\right)^2 + 2e^2 \left|\phi\right|^2 \left(\left(a^1_\mu\right)^2 + \left(a^2_\mu\right)^2 \right) + 2\frac{\Lambda^6}{\left|\phi\right|^2} . \tag{2}$$

The effective gauge coupling e enters into both the effective field strength $G^{a,\mu\nu}_E$ and the mass m for the fields $a^{1,2}_\mu$. One has

$$m^2 = m(T)^2 = m_1^2 = m_2^2 = 4e^2 \left|\phi\right|^2 , \quad m_3^2 = 0 . \tag{3}$$

The gauge mode a^3_μ stays massless on tree-level in the effective theory (adjoint Higgs mechanism). The associated unbroken U(1) gauge freedom is fixed by imposing the Coulomb condition $\partial_i a^3_i = 0$. This corresponds to a completely fixed and *physical* gauge (unitary-Coulomb gauge).

[4] This assumption is actually redundant since Λ can be interpreted as a nonperturbative integration constant, see [8].

[5] This involves an admissible electric center transformation [6, 10].

Let us now give the one-loop expressions for the partial pressures $P_1 = P_2$, and P_3 as exerted by the fluctuating gauge modes a^1_μ,a^2_μ, and a^3_μ, respectively. One has

$$P_3 = 2\frac{\pi^2}{90}T^4\,, \quad P_1 = P_2 = -6\,T\int_0^\infty \frac{k^2 dk}{2\pi^2}\ln\left(1 - e^{-\frac{\sqrt{m^2+k^2}}{T}}\right)\,. \tag{4}$$

Notice that in deriving Eq. (4) the vacuum part in the one-loop expressions for the partial pressures can safely be neglected by virtue of momentum constraints in the effective theory [6], see also below. The total one-loop pressure $P_{\text{1-loop}}$ (exerted by fluctuating modes) is given by $P_{\text{1-loop}} = P_1 + P_2 + P_3$.

The temperature evolution of the coupling e is determined by the relation

$$a = 2\pi e\lambda^{-3/2} \tag{5}$$

and by the (inverted) solution of the (one-loop) evolution equation

$$\partial_a\lambda = -\frac{24\lambda^4 a}{2\pi^6}\frac{D(2a)}{1+\frac{24\lambda^3 a^2}{2\pi^6}D(2a)} \tag{6}$$

where

$$D(a) \equiv \int_0^\infty dx \frac{x^2}{\sqrt{x^2+a^2}}\,\frac{1}{\exp(\sqrt{x^2+a^2})-1}\,, \tag{7}$$

$\lambda \equiv \frac{2\pi T}{\Lambda}$, and $a \equiv \frac{m}{2T}$. Eq. (6) guarantees the invariance of the Legendre transformations between thermodynamical quantities when going from the fundamental to the effective theory. The evolution of e with temperature exhibits a logarithmic pole, $e \propto -\log(\lambda - \lambda_c)$, where $\lambda_c = 13.89$ denotes the critical value of the (dimensionless) temperature, and a plateau setting in for λ slightly larger than λ_c. The value of e at the plateau is $e = \sqrt{8}\pi \sim 8.89$.

In calculating radiative corrections to the free-quasiparticle (one-loop) pressure in a real-time formulation the loop momenta in the effective theory are subject to constraints. The latter emerge due to the existence of a maximal scale $|\phi|$ of resolution[6]. In [9] these constraints were discussed, and we content ourselves with simply quoting them here. First, any propagating gauge mode with four-momentum p cannot be further off its mass-shell then $|\phi|^2$. That is

$$|p^2 - m^2| \leq |\phi|^2 \quad \text{(for a massive mode)}\,, \qquad |p^2| \leq |\phi|^2 \quad \text{(for a massless mode)}\,. \tag{8}$$

Second, the momentum transfer within a vertex needs to be constrained. For a three-vertex (ii) is already contained in (i) by momentum conservation in the vertex. For a four-vertex one needs to distinguish s, t, and u channels in the scattering process.

[6]Since the length scale $|\phi|^{-1}$ is deep inside the saturation regime for the spatial coarse-graining [6, 7] physical quantities should not depend on a mild rescaling of $|\phi|$. We have checked the validity of this assertion when computing the polarization tensor of the massless mode [10].

Suppose that the ingoing (outgoing) momenta are labeled by p_1 and p_2 (p_3 and $p_4 = p_1 + p_2 - p_3$). Then the following three conditions emerge

$$\begin{aligned} |(p_1+p_2)^2| &\leq |\phi|^2\,, \quad (s \text{ channel}) \qquad |(p_3-p_1)^2| \leq |\phi|^2\,, \quad (t \text{ channel}) \\ |(p_2-p_3)^2| &\leq |\phi|^2\,, \quad (u \text{ channel})\,. \end{aligned} \tag{9}$$

For a three-vertex conditions (9) are already contained in (8) by momentum conservation in the vertex. Notice that the three conditions in Eq. (9) reduce to the first condition if one computes the one-loop tadpole contribution to the polarization tensor or the two-loop contribution to a thermodynamical quantity, say the pressure, arising from a four-vertex [11, 10]. Namely, the t-channel condition is then trivially satisfied while the u-channel condition reduces to the s-channel condition by letting the loop momentum $k \to -k$ in $|(p-k)^2| \leq |\phi|^2$, see [6, 10, 11]. Notice also that upon a euclidean rotation $p_0 \to ip_0$ the first condition in(8) goes over in

$$|p^2 + m^2| \leq |\phi|^2\,. \tag{10}$$

For SU(2) the quasiparticle mass is given as $m = 2e\,|\phi|$ with $e \geq \sqrt{8}\pi \sim 8.89$ [6]. Thus condition (10) is never satisfied, and massive modes propagate on-shell only. Conditions (8) and (9) imply that the higher the loop order the more suppressed their contribution to a thermodynamical quantity. General arguments suggest that, apart from diagrams associated with one-particle irreducible resummations of propagators, only a finite number of diagrams contributes to the loop expansion [9]. The main purpose of the present work is to demonstrate the validity of this on the three-loop level.

3 Irreducible three-loop diagrams

We are interested in an estimate for the modulus of each irreducible three-loop diagram contributing to the pressure. By three-loop irreducible we mean that the diagram does not include any line that is dressed by (multiple) insertions of one-loop polarizations. These one-particle reducible contributions to the propagator must be resummed to avoid the occurrence of pinch singularities [9, 10]. Apart from a mild modification of the tree-level propagator this modifies the dispersion law of the associated mode which in turn leads to a slight modifications of the constraints in (8). The claim of [9] is that the loop expansion terminates with respect to irreducible diagrams, that is, with respect to all those diagrams which do not yield a one-particle reducible diagram upon performing a cut (in all possible ways) on a single line.

The only three-loop irreducible diagrams are depicted in Fig 1. In the following we use the convention as in Fig 1 for labelling the loop momenta. For diagrams A, B, and C the number $\tilde{K}$ of independent, potentially noncompact loop variables $(p_0, |\mathbf{p}|)_i$, $(i = 1, 2, 3)$, is $\tilde{K} = 6$, and the number K of independent constraints is $K = 7$. This implies that the support for the loop integrations is either compact or

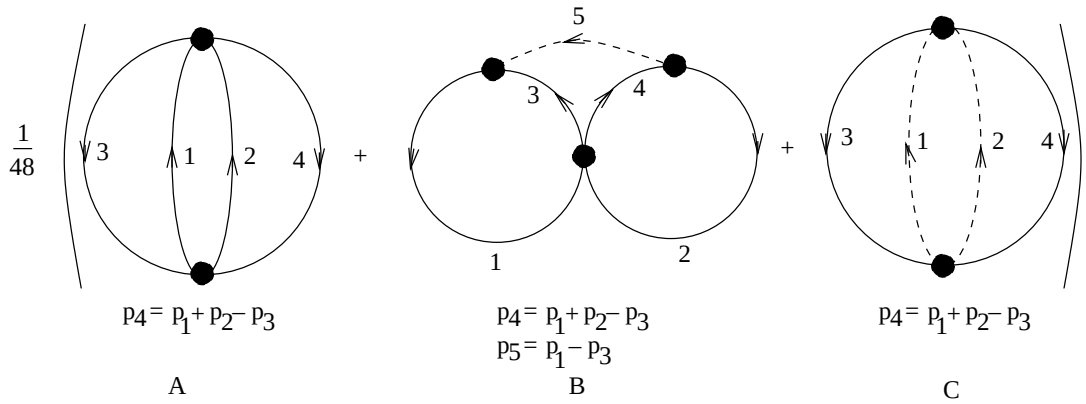

Figure 1: Irreducible three-loop contributions to the pressure. Solid (dashed) lines are associated with the propagators of massive (massless) modes.

empty, see also the discussion in [9]. As we shall see, the former possibility applies to diagrams A and B while diagram C vanishes.

Let us first discuss diagrams A and B. Upon use of the Feynman rules, see [10], considering the symmetry factor $\frac{1}{48}$, by appealing to the triangle inequality, using the fact that the modes $a_\mu^{1,2}$ propagate (on-shell) thermally only, integrating over the time components of the independent loop momenta (momentum conservation), and after a rescaling of the radial components of loop momenta as

$$|\mathbf{p_i}| \to x_i \equiv \frac{|\mathbf{p_i}|}{|\phi|}\,, \quad (i = 1, 2, 3) \tag{11}$$

one arrives at the following estimate for the moduli of the pressure corrections

$\Delta P_A, \Delta P_B$

$$
\begin{aligned}
\left|\Delta P_{A(B)}\right| \;\leq\; & \frac{e^4\Lambda^4\lambda^{-2}}{3\times 2^7\times(2\pi)^6}\sum_{l,m,n=1}^{2}\int dx_1\int dx_2\int dx_3\int dz_{12}\int dz_{13}\int_{z_{23,l}}^{z_{23,u}} dz_{23} \\
& \frac{1}{\sqrt{(1-z_{12}^2)(1-z_{13}^2)-(z_{23}-z_{12}z_{13})^2}}\frac{x_1^2x_2^2x_3^2}{\sqrt{x_1^2+4e^2}\sqrt{x_2^2+4e^2}\sqrt{x_3^2+4e^2}}\times \\
& \delta\left(4e^2+(-1)^{l+m}\sqrt{x_1^2+4e^2}\sqrt{x_2^2+4e^2}-x_1x_2z_{12}-\right. \\
& ((-1)^{l+n}\sqrt{x_1^2+4e^2}\sqrt{x_3^2+4e^2}-x_1x_3z_{13})- \\
& \left.((-1)^{m+n}\sqrt{x_2^2+4e^2}\sqrt{x_3^2+4e^2}-x_2x_3z_{23})\right)\times \\
& \left|\mathcal{P}_{A(B)}(\mathbf{x},\mathbf{z},l,m,n)\right| \; n_B\left(2\pi\lambda^{-3/2}\sqrt{x_1^2+4e^2}\right)\times \\
& n_B\left(2\pi\lambda^{-3/2}\sqrt{x_2^2+4e^2}\right)\; n_B\left(2\pi\lambda^{-3/2}\sqrt{x_3^2+4e^2}\right)\times \\
& n_B\left(2\pi\lambda^{-3/2}\left|(-1)^l\sqrt{x_1^2+4e^2}+(-1)^m\sqrt{x_2^2+4e^2}+(-1)^n\sqrt{x_3^2+4e^2}\right|\right)\,,
\end{aligned}
\tag{12}
$$

where $z_{12}\equiv\cos\angle(\mathbf{x}_1,\mathbf{x}_2)$, $z_{13}\equiv\cos\angle(\mathbf{x}_1,\mathbf{x}_3)$, and $z_{23}\equiv\cos\angle(\mathbf{x}_2,\mathbf{x}_3)$. The functions $\mathcal{P}_A$, $\mathcal{P}_B$ emerge from Lorentz and color contractions and are regular at $x_1=x_2=x_3=0$ (mass gap for $a_\mu^{1,2}$). We refrain from quoting them here explicitly for environmental reasons[7]. In addition, we define:

$$
z_{23,u}\equiv\cos\left|\arccos z_{12}-\arccos z_{13}\right|\,,\quad z_{23,l}\equiv\cos\left|\arccos z_{12}+\arccos z_{13}\right|\,. \tag{13}
$$

The integrations in Eq. (12) are subject to the following constraints (see (8) and (9)):

$$
\begin{aligned}
z_{12} &\leq \frac{1}{x_1x_2}\left(4e^2-\sqrt{x_1^2+4e^2}\sqrt{x_2^2+4e^2}+\frac{1}{2}\right)\equiv g_{12}(x_1,x_2)\,,\\
z_{13} &\geq \frac{1}{x_1x_3}\left(-4e^2+\sqrt{x_1^2+4e^2}\sqrt{x_3^2+4e^2}-\frac{1}{2}\right)\equiv g_{13}(x_1,x_3)\,,\\
z_{23} &\geq \frac{1}{x_2x_3}\left(-4e^2+\sqrt{x_2^2+4e^2}\sqrt{x_3^2+4e^2}-\frac{1}{2}\right)\equiv g_{23}(x_2,x_3)\,.
\end{aligned}
\tag{14}
$$

Notice that for diagram B the constraint (8) for the momentum $p_5=p_1-p_3$ of the massless mode is the same as the t-channel constraint for the four-vertex. Therefore

[7]Upon request the reader will be provided with the Mathematica notebooks containing the functions $\mathcal{P}_A$, $\mathcal{P}_B$ in explicit form.

no extra condition for the (off-shell) momentum p_5 is needed. According to the investigation in [9] the conditions (14) together with Eq. (13) imply that the support for the integration in x_1, x_2, and x_3 is contained in the compact set $\{x_1, x_2, x_3 < 3\}$.

Let us now turn to diagram C. We first consider the case that the momenta p_1 and p_2 of the massless modes, compare Fig. 1, are both off-shell within the constraints dictated by (8). In analogy to diagrams A and B one then derives that

$$\begin{aligned} |\Delta P_C| \;\leq\; & \frac{e^4\Lambda^4\lambda^{-2}}{3\times 2^5\times(2\pi)^8}\sum_{l,m=1}^{2}\int dy_1\int dx_1\int dx_2\int dx_3\int dz_{12}\int dz_{13}\int_{z_{23,l}}^{z_{23,u}} dz_{23} \\ & \frac{x_1^2x_2^2x_3^2}{\sqrt{(1-z_{12}^2)(1-z_{13}^2)-(z_{23}-z_{12}z_{13})^2}}\,|\mathcal{P}_C(\mathbf{x},\mathbf{z},y_1,l,m)|\times \\ & n_B\left(2\pi\lambda^{-3/2}\sqrt{x_3^2+4e^2}\right)\,\frac{n_B\left(2\pi\lambda^{-3/2}\left|(-1)^l\sqrt{x_3^2+4e^2}+(-1)^m f_2(\mathbf{x},\mathbf{z})\right|\right)}{f_2(\mathbf{x},\mathbf{z})\sqrt{x_3^2+4e^2}}\,, \end{aligned} \tag{15}$$

where

$$\begin{aligned} f_2(\mathbf{x},\mathbf{z}) &\equiv \sqrt{x_1^2+x_2^2+x_3^2+2x_1x_2z_{12}-2x_1x_3z_{13}-2x_2x_3z_{23}}\,, \\ y_1 &\equiv \frac{p_1^0}{|\phi|}\,, \end{aligned} \tag{16}$$

and $z_{23,l}$, $z_{23,u}$ are defined as in Eq. (13). The function $\mathcal{P}_C$ emerges from Lorentz and color contractions and is regular at $x_1 = x_2 = x_3 = 0$ (mass gap for $a_\mu^{1,2}$). The integrations in Eq. (15) are subject to the following constraints

$$\begin{aligned} 1 &\geq |y_1^2+y_2^2-x_1^2-x_2^2+2y_1y_2-2x_1x_2z_{12}|\,, \\ 1 &\geq |y_2^2-x_2^2+4e^2-(-1)^l 2y_2\sqrt{x_3^2+4e^2}+2x_2x_3z_{23}|\,, \\ 1 &\geq |y_1^2-x_1^2+4e^2-(-1)^l 2y_1\sqrt{x_3^2+4e^2}+2x_1x_3z_{13}|\,, \\ 1 &\geq |y_1^2-x_1^2|\,, \qquad 1\geq |y_2^2-x_2^2|\,, \end{aligned} \tag{17}$$

where

$$y_2 = -y_1 + 2(-1)^l\sqrt{x_3^2+4e^2}+(-1)^m\,f_2(\mathbf{x},\mathbf{z})\,. \tag{18}$$

As we shall see in Sec. 4, the constraints in (17) imply that the support for the integration in Eq. (15) is empty. As a consequence, the cases that one or both of the massless modes in diagram C propagate on shell also have an empty support. This is because the conditions $|p_1^2|, |p_2^2| \leq |\phi|^2$, which went into (17), contain the cases $p_1^2 = 0$ and/or $p_2^2 = 0$. Thus diagram C is the first example of an vanishing irreducible diagram in the loop expansion. As was argued in [9] one expects that the number of such cases will drastically increase with increasing loop numbers.

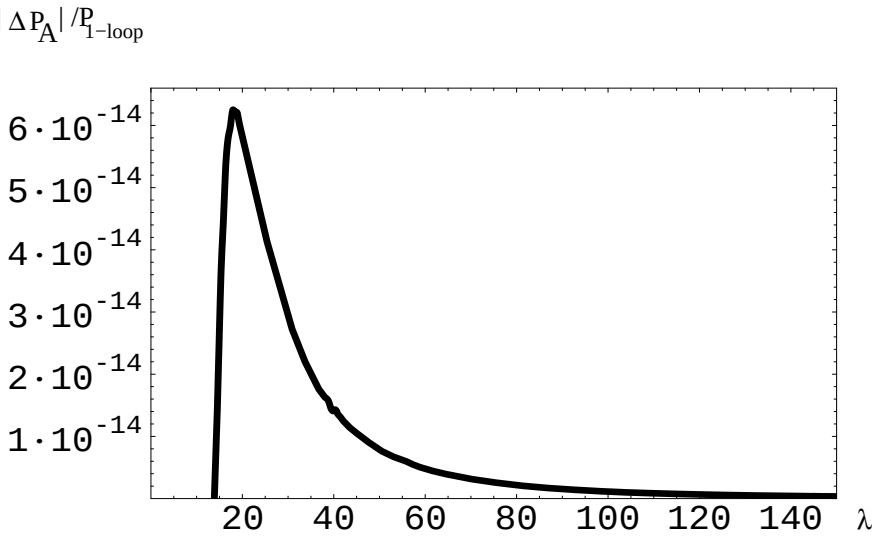

Figure 2: An upper estimate for the modulus of the pressure contribution $|\Delta P_A|$ due to diagram A in Fig. 1. The plot shows this estimate normalized to the one-loop result $P_{\text{1-loop}}$, see Eq. (4).

4 Numerical evaluation and results

Here we present our results obtained by using the Monte-Carlo method of integration for the regular integrands[8] of Eqs. (12) and (15). Let us first discuss diagrams A and B. It is known [9] that the support in x_2, x_3 for the integral in Eqs. (12) is contained in the compact set $\{x_2, x_3 < 3\}$ while the support for the integration in z_{12}, z_{13}, z_{23} naturally is contained in the set $\{-1 \leq z_{12}, z_{13} \leq +1; z_{23,l} \leq z_{23} \leq z_{23,u}\}$, see Eq. (13). Points are thus chosen randomly in the union of these two compact sets. Any point that satisfies the constraints (14) contributes to the integrals. We have worked with a sample size of 5×10^5 points, and we have observed a typical statistical uncertainty of about 1% in our results. In Fig. 2 our estimate for $\frac{|\Delta P_A|}{P_{\text{1-loop}}}$ is shown as a function of (dimensionless) temperature. Notice the sudden drop to zero near $\lambda_c = 13.87$ which is due to the decoupling of the massive modes $a_\mu^{1,2}$. The functional shape is similar to that of the modulus of the leading two-loop correction: There is a maximum at $\lambda \sim 20$ and a very rapid decay to the right of this maximum. Notice, however, that the value of the maximum is suppressed by a factor of about 10^{-7} as compared to the smallest two-loop correction [10]. In Fig. 3 we present our estimate for $\frac{|\Delta P_B|}{P_{\text{1-loop}}}$ as a function of (dimensionless) temperature. The maximum of this contribution is comparable to the smallest two-loop correction.

For diagram C we have chosen a compact set $\{x_1, x_2, x_3 \leq R, -R \leq y_1 \leq R, -1 \leq z_{12}, z_{13} \leq +1; z_{23,l} \leq z_{23} \leq z_{23,u}\}$ in which the Monte-Carlo method samples points. We have varied R in the range $0.1 \leq R \leq 15$ and have used samples with up to 6×10^8 points. We have not found any point which satisfies all of the conditions (17). This is physically suggestive since the diagram describes annihilation or creation of two massive on-shell modes into or out of two massless off-shell modes. Typically,

[8]The x_1-integration is performed analytically in order to eliminate the δ-function in the original integrand. There are eight zeros of the argument of the δ-function in x_1 some of which turn out to be complex and thus can be discarded.

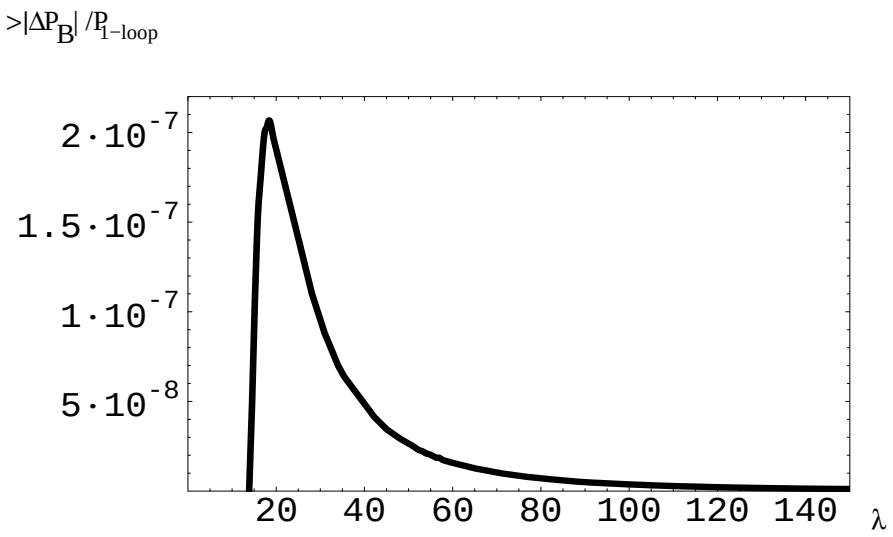

Figure 3: An upper estimate for the modulus of the pressure contribution $|\Delta P_B|$ due to diagram A in Fig. 1. The plot shows this estimate normalized to the one-loop result $P_{\text{1-loop}}$, see Eq. (4).

the off-shellness of a massless modes is comparable to the mass of the massive mode. This very fact, however, is in stark contradiction with condition (8). At loop order three we thus have found a first example of an irreducible loop diagram that vanishes. We expect that this situation occurs very frequently at higher loop orders, see discussion in [9].

5 Conclusions

In this paper we have performed estimates on the moduli of the three irreducible three-loop diagrams which contribute to the pressure of a thermalized SU(2) Yang-Mills theory being in its deconfining phase. Our results are consistent with the general arguments in [9] which imply a rapid convergence of the loop expansion. Namely, one of these three diagrams vanishes exactly because the constraints on the loop momenta, which emerge in the effective theory, imply that the support for the integration is empty. So the situation that an irreducible diagram is precisely zero, which in [9] is argued to occur at a finite loop order, takes place at three-loops for the first time. Moreover, we observe that the modulus of the dominating three-loop diagram is comparable to that of the smallest two-loop diagram and by a factor of $\sim 10^{-4}$ suppressed as compared to the dominating two-loop diagram [10]. The modulus of the other nonvanishing, irreducible three-loop diagram is by a factor of $\sim 10^{-11}$ suppressed as compared to the dominating two-loop diagram.

Acknowledgments

We would like to thank Markus Schwarz for useful conversations and helpful comments on the manuscript. One of us (R.H.) acknowledges fruitful discussions with Francesco Giacosa.

References

[1] G. 't Hooft and M. J. G. Veltman, Nucl. Phys. B **44**, 189 (1972).
G. 't Hooft, Nucl. Phys. B **33**, 173 (1971).
G. 't Hooft, Nucl. Phys. B **62**, 444 (1973).
G. 't Hooft and M. J. G. Veltman, Nucl. Phys. B **50**, 318 (1972).

[2] D. J. Gross and Frank Wilczek, Phys. Rev. D **8**, 3633 (1973).
D. J. Gross and Frank Wilczek, Phys. Rev. Lett. **30**, 1343 (1973).
H. David Politzer, Phys. Rev. Lett. **30**, 1346 (1973).
H. David Politzer, Phys. Rept. **14**, 129 (1974).

[3] A. D. Linde, Phys. Lett. B **108**, 389 (1982).
A. M. Polyakov, Phys. Lett. B **59**, 82 (1975).

[4] F. Giacosa and R. Hofmann, hep-th/0703127.

[5] A. M. Polyakov, Phys. Lett. B **59**, 82 (1975).
C. P. Korthals Altes, hep-ph/0406138, hep-ph/0408301.
C. P. Korthals Altes, Acta Phys. Polon. B **34**, 5825 (2003).
P. Giovannangeli and C. P. Korthals Altes, Nucl. Phys. B **608**, 203 (2001).
C. Korthals-Altes, A. Kovner, and M. A. Stephanov, Phys. Lett. B **469**, 205 (1999).

[6] R. Hofmann, Int. J. Mod. Phys. A**20** (2005) 4123, Erratum-ibid. A **21** (2006) 6515.
R. Hofmann, Mod. Phys. Lett. A**21**, 999 (2006), Erratum-ibid. A **21**, 3049 (2006).

[7] U. Herbst and R. Hofmann, hep-th/0411214.

[8] F. Giacosa and R. Hofmann, hep-th/0609172.

[9] R. Hofmann, hep-th/0609033.

[10] M. Schwarz, R. Hofmann and F. Giacosa, Int. J. Mod. Phys. A**22**, 1213 (2007).

[11] U. Herbst, R. Hofmann, J. Rohrer, Acta Phys. Pol. B**36**, 881 (2005).